Slow Calcium Signals after Tetanic Electrical Stimulation in Skeletal Myotubes

José M. Eltit, Jorge Hidalgo, José L. Liberona, and Enrique Jaimovich
Centro de Estudios Moleculares de la Célula, Instituto de Ciencias Biomédicas, Facultad de Medicina, Universidad de Chile, Santiago, Chile

ABSTRACT The fluorescent calcium signal from rat myotubes in culture was monitored after field-stimulation with tetanic protocols. After the calcium signal sensitive to ryanodine and associated to the excitation-contraction coupling, a second long-lasting calcium signal refractory to ryanodine was consistently found. The onset kinetics of this slow signal were slightly modified in nominally calcium-free medium, as were both the frequency and number of pulses during tetanus. No signal was detected in the presence of tetrodotoxin. The participation of the dihydropyridine receptor (DHPR) as the voltage sensor for this signal was assessed by treatment with agonist and antagonist dihydropyridines (Bay K 8644 and nifedipine), showing an enhanced and inhibitory response, respectively. In the dysgenic GLT cell line, which lacks the $\alpha 1_S$ subunit of the DHPR, the signal was absent. Transfection of these cells with the $\alpha 1_S$ subunit restored the slow signal. In myotubes, the inositol 1,4,5-trisphosphate (IP_3) mass increase induced by a tetanus protocol preceded in time the slow calcium signal. Both an IP_3 receptor blocker and a phospholipase C inhibitor (xestospongin C and U73122, respectively) dramatically inhibit this signal. Long-lasting, IP_3-generated slow calcium signals appear to be a physiological response to activity-related fluctuations in membrane potential sensed by the DHPR.

INTRODUCTION

The voltage-sensitive calcium channels belong to the ion channel super-family that includes K^+ and Na^+ selective channels as well. The pharmacological and electrophysiological diversity of these calcium channels is due mainly to the abundance of the $\alpha 1$ subunit isoforms and their association to a manifold of modulating subunits. In mammals, >10 different genes encode for isoforms of the $\alpha 1$ subunit (Catterall, 2000). Historically, these channels have been classified according to the type of calcium current, its specific blocker, or its location. In skeletal muscle, the Cav1.1 calcium channel, also called $\alpha 1_S$ or dihydropyridine receptor (DHPR), is the main type present. Electrophysiologically it can be characterized by the L-type current and presents binding sites for dihydropyridines (Ertel et al., 2000; Catterall, 2000). The DHPR molecule was first purified from the transverse tubule (T tubule) of skeletal muscle (Curtis and Catterall, 1984). The whole receptor is a pentamer and the main subunit is the $\alpha 1$ subunit, whose structure resembles the pore forming subunit of the Na^+ channel (Catterall, 2000; Wolf et al., 2003). Although most of the membrane potential sensor studies have been done in either Na^+ or K^+ channels, the molecule domains involved in the voltage sensor are conserved in all of the voltage-gated cation channels and this knowledge can be extrapolated to the calcium channel (Catterall, 2000).

Address reprint requests to Enrique Jaimovich, Centro de Estudios Moleculares de la Célula, Instituto de Ciencias Biomédicas, Facultad de Medicina, Universidad de Chile, Casilla 70005, Independencia 1027, Santiago 6530499, Chile. Tel.: 562-678-6510; Fax: 562-735-3510; E-mail: ejaimovi@med.uchile.cl.

The movement of the charged residues evidenced by the gating current gives support to the notion of a conformational change in the protein that shifts the open channel probability during membrane depolarization. This change is relevant during the T tubule depolarization and allows for the cross-talk between the DHPR and ryanodine receptor (RyR) (located in the sarcoplasmic reticulum), which is associated to the excitation-contraction (EC) coupling mechanism. Cumulative evidence demonstrates that the II-III loop of $\alpha 1_S$ is the site of physical interaction between the DHPR and RyR1 (Tanabe et al., 1990; Grabner et al., 1999; Proenza et al., 2002).

A detailed study of high potassium depolarization-induced calcium signals in myotubes has shown that, in addition to the well-established ryanodine-sensitive (fast) calcium signal related to EC coupling, there is a second (slow) calcium signal, which is refractory to ryanodine and it has besides the cytoplasmic component a marked nuclear component (Jaimovich et al., 2000; Estrada et al., 2001). The fast and slow signals share their dependency on DHPR activation as well as being independent of extracellular calcium. Thus, the calcium released in both situations originates from intracellular stores. When high potassium is used as the depolarization activator, the onset of the slow calcium signal is inhibited by the presence of either U73122 (phospholipase C (PLC) inhibitor), xestospongin C (inositol 1,4,5-trisphosphate receptor (IP_3R) blocker), or 2-aminoetoxiphenil borate. These results suggest the involvement of IP_3R in the slow calcium signal (Estrada et al., 2001).

The cytosolic increase of IP_3 and diacylglycerol must reflect PLC activity and as a consequence, the elicited IP_3 will activate the release of Ca^{2+} from intracellular stores as a depolarization-dependent process. In addition, it will prime Ca^{2+}-dependent metabolic pathways, such as extracellular

signal-regulated kinase phosphorylation, increased by depolarization (Powell et al., 2001; Carrasco et al., 2003). These results indicate that in muscle cells there are at least two calcium releasing mechanisms activated by depolarization, a fast one linked through RyR to EC coupling and a slow one, mediated by IP_3, which is detectable in the nucleus as well as in the cytoplasm. Therefore, the differential localization of IP_3 receptors will provide for a differential signaling response to depolarization events, particularly if the depolarization signal, as it occurs in muscle, has the distinct feature of being repetitive in nature with varying frequencies. The physiological role of the slow calcium signal in the nucleus remains to be clarified, but it appears to be involved in the activation of transcription factors and the eventual control of gene expression mediated by calcium (Carrasco et al., 2003).

In this work we present a detailed study of the calcium signaling evoked by an extracellular field electrical stimulation. We performed the procedure using electrical rather than high potassium stimulation, because it yields a closer representation of the physiological condition found during tetanic stimulation. We tested the hypothesis whether DHPR as a voltage sensor (Araya et al., 2003) is mediating both types of calcium signals, the fast one dependent on RyR and the slow one evoked through PLC activation.

MATERIALS AND METHODS

Cell cultures

Neonatal rat myotubes were cultured as previously described by Jaimovich et al. (2000). Briefly, muscle tissue from the hind limbs of from 12- to 24-h postnatal rat pups was mechanically dispersed and then treated with 0.2% (wt/vol) collagenase for 15 min at mild agitation. The suspension was filtered through Nytex membrane or lens tissue paper and spun down at low speed. A 10- to 15-min preplating was done for enrichment of myoblasts, then cells were plated at densities of 3.5×10^5/dish (35 mm) and 9.5×10^5/dish (60 mm) for Ca^{+2} measurements and IP_3 binding, respectively. Plating media was DMEM-Ham's F-12, 10% bovine serum, 2.52% fetal calf serum, 100 mg/l penicillin, 50 mg/l streptomycin, and 2.5 mg/l amphotericin B. For fluorescence measurements, the cells were plated on round coverslips pretreated with a 1% gelatin solution placed in the culture dishes for 30 min. To eliminate remaining fibroblasts, 10 μM of cytosine arabinoside was added at the third day of culture. After 36 h in culture, fetal calf serum concentration was reduced to 1.8% (vol/vol) to induce differentiation. Myotubes in the dish, some spontaneously contracting, with an estimated purity >90%, were visible after the fifth day of culture and they were used for experiments after 6–8 days in culture. DMEM-F12 medium, bovine serum, and fetal bovine serum were from GIBCO BRL (Carlsbad, CA). Cytosine arabinoside, penicillin, streptomycin, and amphotericin B were from Sigma-Aldrich (St. Louis, MO).

Cell lines

We used the mutant mouse cell line GLT (muscular dysGenic, *mdg/mdg,* line transfected with the large T antigen), and the wild-type muscle cell line NLT, prepared from dysgenic and normal littermate cultures, respectively (Powell et al., 1996). A GLT-α1 cell line was derived from a stable-transfected clone of the GLT cell with the $\alpha 1_S$ DHPR subunit that was selected by neomycin resistance as recently described in our laboratory by Araya et al (2003). The expression of the $\alpha 1_S$-DHPR subunit in the GLT-α1 cell line was studied by Western blot and immunohistochemistry (Araya et al., 2003). We also used the 1B5 cell line, which was a generous gift from Dr. Paul Allen. The 1B5 cells were allowed to grow to 50–80% confluence and then the serum composition of the medium was changed to 2% horse serum to induce cell differentiation and fusion to yield multinucleated myotubes. Cells were plated following the same procedures used for primary cultured myotubes.

Cell pretreatment

Before a specific experiment, the cells were incubated from 30 to 60 min with 10 μM tetrodotoxin (TTX) (Sigma-Aldrich), 10–30 μM ryanodine (Sigma-Aldrich), 1 μM nifedipine (Sigma-Aldrich), 2 μM (−)S-Bay K 8644 (RBI, Natick, MA), 5 μM xestospongin C (Calbiochem, La Jolla, CA), or 30 μM U73122 (Sigma-Aldrich), in Krebs buffer (145 mM NaCl, 5 mM KCl, 1 mM $CaCl_2$, 1 mM $MgCl_2$, 10 mM HEPES-Na, 5.6 mM glucose, pH 7.4). Then, the cells were loaded with fluo-3-acetoximethylester (Fluo-3 AM, Molecular Probes, Eugene, OR) in the Krebs buffer in the presence of the given pharmacological agent for another 20 min. The coverslips were mounted in a 1-ml capacity chamber and washed three times and incubated in Krebs solution (also in the presence of the drug) leaving the cells ready for stimulation. Alternatively, for the free calcium condition, after incubation with the dye and washout, the cells were switched to a free-calcium saline (145 mM NaCl, 5 mM KCl, 0.5 mM EGTA, 2 mM $MgCl_2$, 10 mM HEPES-Na, 5.6 mM glucose, pH 7.4). For the control condition, cells were subjected to the same procedure but only with vehicle instead of the drug.

ELECTRICAL STIMULATION

Slow calcium signal acquisition

The 1-ml chamber with the cells was placed in the stage of an inverted microscope equipped with epifluorescence illumination by a 100-W mercury lamp (Olympus T041, New Hyde Park, NY). The side port is connected to a CCD cooled camera (MCD600, Spectra Source Instruments, Westlake Village, CA); the full or partial image acquisition is computer-controlled through macros that operate the software provided by the manufacturer. The same program controls the generation of the electrical pulse train by a stimulator in which the modifications of frequency, number of pulses, duration of each pulse, and intensity are easily controlled. These pulses were delivered to the dish by a pair of platinum electrodes placed within 3 mm of each other. The electrode assembly is set 1–2 mm over the cells with a micromanipulator, leaving those that are in focus between the two wires. A filter wheel (Lambda 10-2, Sutter Instruments, Novato, CA) works as a shutter of fluorescence illumination and is also controlled by the image acquisition software. In this system we cannot capture images during the tetanic stimulation, so that the shutter was always in the closed position and once the protocol of stimulation ended, a sequence of 80 images, each of 200-ms exposure, were acquired every 6.6 s. Thus illumination was limited to the exposure time plus some mechanical timing overhead, which allowed the lowest possible rate of dye bleaching. Image processing was done off-line with the public domain ImageJ software (Rasband,

1997); curvefitting and graphs were performed with Origin 6.0 (OriginLab, Northampton, MA).

Fast calcium signal measurements

For the acquisition of the calcium signal during the tetanus stimulation, the CCD camera is inadequate. So the light corresponding to the center of the visual field of the microscope was collected on the side port of the microscope by an optic fiber and attached to a photodiode amplifier assembly whose output was connected to an A/D converter (Labmaster DMA, Scientific Solutions, Mentor, OH). The rise time for this system is 0.5 ms; therefore, in these experiments the output was filtered to 2 KHz with an 8-pole Bessel filter (Frequency Devices, Haverhill, MA) and digitized at 10 KHz. In this way, we were able to sample the fast fluorescent transients from a cell during a single pulse or a tetanus protocol.

Measurements of IP_3 mass changes in response to electrical stimulation

The IP_3 mass measurement was performed in myotubes cultured in 60-mm dishes. To obtain a homogeneous electrical stimulation of all the cells in the dish, we built a stimulation device that consists of a row of six platinum wires intercalated 1 cm apart with alternate polarity across a circular plastic holder that fits in the dish. The two terminals were connected to a stimulator unit with manual control of the frequency, intensity, and duration of each pulse. The square pulses were monitored displaying the signal in an oscilloscope. To verify the effectiveness of this stimulation system, the cells were subjected to low frequency stimulation (0.2 Hz) and the generalized cell contraction was visually monitored under the microscope. This electrode arrangement can induce an effective cell contraction in $>85\%$ of the cells in the dish.

The IP_3 measurement was performed as previously described by Jaimovich et al. (2000). Briefly, myotubes were rinsed and preincubated for 20 min in Krebs buffer; after the electrical stimulation, at the times indicated, the Krebs buffer was aspired, followed by the addition of 0.8 M ice-cold perchloric acid, and freezing with liquid nitrogen. Samples were allowed to thaw and cell debris was spun down for protein determination (Hartree, 1972). The supernatant was neutralized with a solution of 2 M KOH, 0.1 M 2-[*n*-morpholinoethanesulfonic] acid, and 15 mM ethylenediaminetetraacetic acid (EDTA). These extracts were kept frozen until required for IP_3 mass determination by a radio-receptor assay (Liberona et al., 1998). Briefly, a crude rat cerebellum membrane preparation was obtained after homogenization in 50 mM Tris-HCl, pH 7.7, 1 mM EDTA, 2 mM β-mercaptoethanol, and centrifugation at 20,000 $\times$ *g* for 15 min. This procedure was repeated three times, and the final pellet was resuspended in the same solution plus 0.3 M sucrose and then frozen at $-80°C$ until use. The membrane preparation was calibrated for IP_3 binding with 1.6 nM ^{3}H-IP_3 (D-[2-^{3}H]-*myo*-inositol 1,4,5-trisphosphate), specific activity 21.0 Ci/mmol (DuPont/NEN, Boston, MA), and 2–120 nM cold IP_3 (Sigma-Aldrich). The sample analysis was performed in a similar way but an aliquot of the neutralized supernatant was added instead of cold IP_3. The ^{3}H-IP_3 radioactivity remaining bound to the cerebellar membranes was measured in a Beckman LS-6000TA liquid scintillation spectrometer (Beckman Instruments, Fullerton, CA).

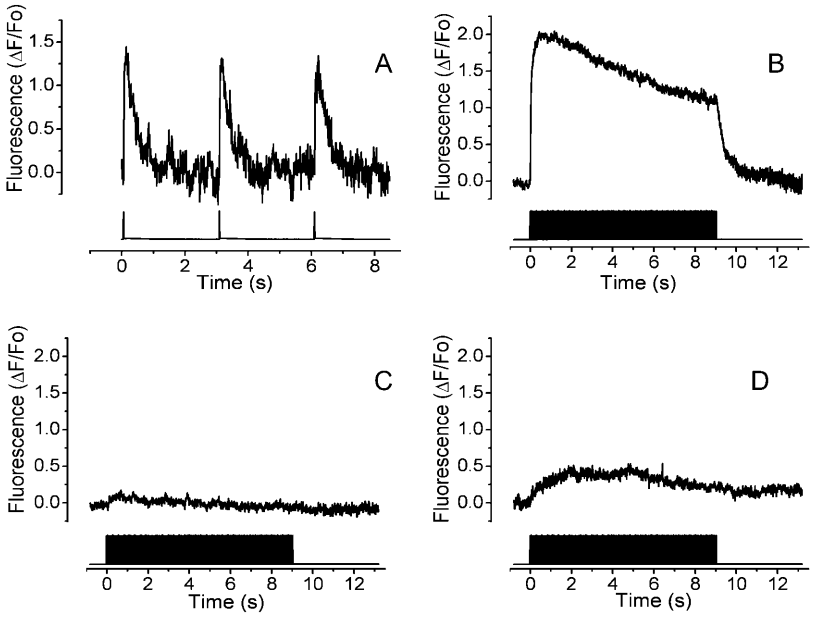

FIGURE 1 Electrical field stimulation by single pulses elicits a rapid calcium signal in skeletal myotubes. The fluorescence was monitored by a photodiode attached to the side port of the microscope. The top trace shows the calcium transient and the bottom trace shows the electrical pulses. (*A*) Representative record of myotubes stimulated with 1-ms pulses at 0.33 Hz. (*B*) Control calcium transient induced by 400 pulses of 1 ms each at 45 Hz. The mean trace of 13 experiments is shown. (*C*) The same stimulation as in *B* but in the presence of 10 μM of TTX. The mean trace of 13 experiments is shown. (*D*) The same stimulation described in *B*; in cells preincubated with 30 μM of ryanodine. The mean trace of 10 experiments is shown.

Image and data analysis

The captured image sequence for an experiment was baseline corrected by subtraction of a prestimulus fluorescent image. The mean intensity of a 25 × 25 pixel region of interest located either in the nucleus or the cytoplasm was collected to represent $F(t)$. The signal was normalized as $\{F(t)-F(0)\}/F(0)$ and fitted to the logistic function providing values for maximum fluorescence and half-time for rise, $t_{1/2}$. The photodiode signal from the falling phase of a single transient was fitted to a single exponential decay function. Data of n experiments were expressed as mean ± SE and analyzed by unpaired Student's t-test, and one-way ANOVA followed by the Dunnet's post test. A P value <0.05 was considered to be statistically significant.

RESULTS

Electrical pulses induce a TTX and ryanodine-sensitive fast calcium signal

Single twitch events were obtained by a low-frequency (0.33 Hz) 1-ms stimulus protocol. Fig. 1 *A* shows the single calcium transients obtained with such protocol. The shape of this calcium transient closely corresponds to those previously reported (Kubis et al., 2003; Kasielke et al., 2003). Kinetically, the calcium transient induced by low-frequency stimulation has a single exponential decay with a time constant of 0.325 ± 0.019 s (Table 1). At a higher frequency of stimulation (45 Hz, Fig. 1 *B*) the calcium fluorescence initially peaked to 2.01 ± 0.19 $\Delta F/F_o$; then the plateau decayed slowly during the stimulation protocol (9 s). Once the stimulation was over, calcium decreased to basal levels with a time course that shows no statistical difference when compared to that for a single pulse. The fact that there are no differences in decay kinetics implies that the mechanisms for intracellular calcium store refilling were not altered by the high-frequency stimulation. To verify that the electrical protocol induced action potentials that in turn activated the intracellular calcium release mechanism, the voltage-dependent sodium channels were blocked with TTX. Under these conditions, there is no calcium rise induced by either the 0.33-Hz or the 45-Hz stimulation protocols (14 and 13 total inhibition, respectively, out of a total of 15 experiments for each condition, Fig. 1 *C*). To define whether in our experimental conditions the action potentials activated a RyR-dependent intracellular calcium release, we exposed myotubes to 30 μM ryanodine, a concentration that is inhibitory of release through its receptor. Under these conditions, close to 80% of the calcium signal was blocked (Fig. 1 *D*).

TABLE 1 Parameters for the decay of the calcium transient

Frequency (Hz)	$(\Delta F/F_o)_{max}$	Decay time constant τ (s)
0.33	1.48 ± 0.14	0.325 ± 0.019
45	2.01 ± 0.19	0.439 ± 0.068

No significant differences were found ($n = 5$).

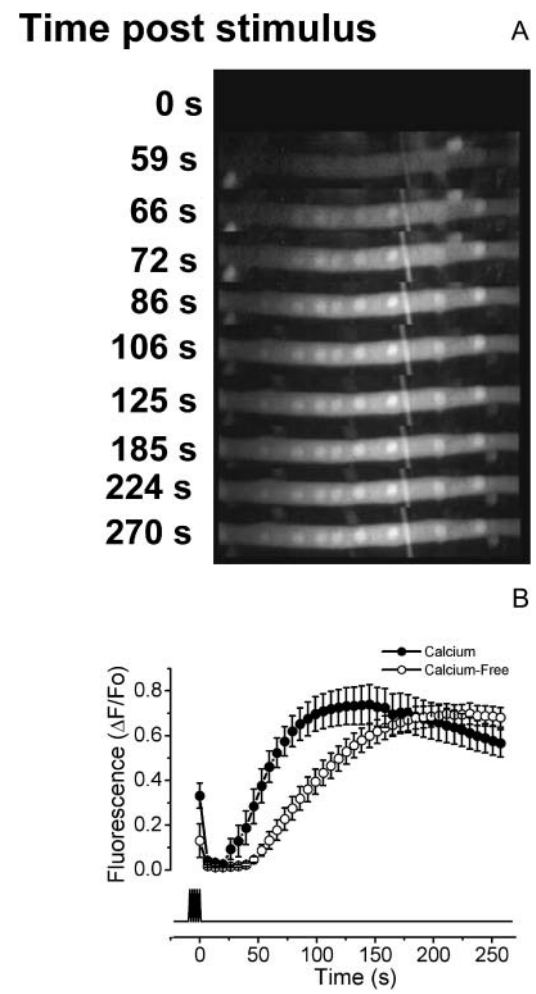

FIGURE 2 Slow calcium signal induced by electrical field stimulation. A sequence of images was taken with the CCD camera attached to the epifluorescence microscope side port equipped with the correct filters to capture the Fluo-3 AM fluorescence to monitor the intracellular Ca^{+2} level. The fast calcium transient is not shown because the images were taken after the end of the stimulus, but in some cases, the tail of the fast component is visualized. The cells were stimulated with 400 pulses of 1 ms each at 45 Hz. The overall signal transient may last nearly 5 min. (*A*) Increase of intracellular calcium induced by electrical stimulation when the cell is in nominal free extracellular calcium (0 calcium saline plus 0.5 mM EGTA). (*B*) The quantification of the slow calcium signal in the presence (*solid circles*) and absence (*open circles*) of extracellular calcium. The analyzed regions of interest were from nuclear zones of the cells and were quantified with ImageJ software. The mean of 12 independent experiments ± SE is shown and the bottom trace shows the moment of the stimulus application.

Slow calcium signal induced by electrical stimulation

As described above, during electrical stimulation the myotubes show a fast calcium transient that appears to be mediated by RyR activation. Once the stimulus is over, calcium rapidly returns to the basal level, but a few seconds

later, a long lasting calcium signal starts to rise (Fig. 2 *A*). The nuclear regions show a slightly higher fluorescence than the cytoplasmic region during this slow calcium transient but kinetically, nuclear and cytoplasmic components show the same behavior. A likely source for this difference may be explained by a dissimilar distribution of Fluo-3 between both compartments. In this work, the signal from a nuclear region of interest was routinely used. When the cells were stimulated with 400 pulses of 1 ms duration at 45 Hz, the slow calcium signal shows a half-time ($t_{1/2}$) for maximal calcium increase of 54.34 ± 4.56 s in the presence of extracellular calcium and of 98.40 ± 7.92 s in the nominally calcium-free saline (Fig. 2 *B*, Table 2). The maximal fluorescence change reached was very similar in both conditions (0.735 ± 0.079 and 0.733 ± 0.046 $\Delta F/F_o$ for calcium and calcium-free media, respectively). The presence or absence of chamber perfusion did not alter significantly the slow calcium signal, indicating that the amount of perturbation produced by the field stimulation was local and transient.

To identify a relationship between the stimulation protocols and the slow calcium signal, cells were exposed to 400 (1-ms) pulses at three different frequencies (10, 45, and 90 Hz; Fig. 3 *A*). All these experiments were performed in the absence of extracellular calcium. Interestingly, both at 10 and 90 Hz there is a similar response with a $t_{1/2}$ of 51.03 ± 21.62 and 49.30 ± 3.14 s, respectively; both kinetics are faster than those found at 45 Hz.

When the cells were stimulated with a different number of pulses (100, 400, or 600 pulses at 45 Hz), the slow calcium transient increased its rate of rise, as in a dose-dependent event (Fig. 3 *B*). The stimulation with 100 pulses, apart from a small tail signal, did not show a slow response. On the other hand, at 400 and 600 pulses, $t_{1/2}$ values of 98.40 ± 7.92 and 28.31 ± 1.57 s were found and the maximal fluorescence increased by 51.3% (from 0.733 ± 0.046 to 1.109 ± 0.069 $\Delta F/F_o$). These results point toward a functional relationship between the putative membrane depolarization sensor and the slow calcium response with a threshold level for the number of depolarizing events required to elicit the response.

The slow calcium signal was blocked by TTX and was insensitive to ryanodine

As shown above, during high-frequency stimulation the cells triggered action potentials. To block the action potential generation by the field stimulation, the cells were exposed to 10 μM TTX in the presence of extracellular calcium. In this series of experiments the slow calcium signal was completely absent (Fig. 4 *A*), suggesting that the action potential and not the extracellular electrical stimulation by itself is the trigger for the slow calcium signal. To study the role of RyRs in calcium release from intracellular stores during the slow calcium signal, cells were exposed to 10 and 30 μM ryanodine in the absence of extracellular calcium. Neither 10 nor 30 μM ryanodine affected the slow calcium signal (Fig. 4 *B*). Moreover, the latter shows a slightly enhanced slow calcium response. An additional source of evidence to support the notion that RyR was not involved in the slow calcium signal came from the electrical stimulation of cells from the 1B5 line, where the slow calcium signal was still present (data not shown).

The DHPR is the membrane potential sensor for the slow calcium signal

When primary myotubes were exposed to nifedipine in a calcium-free medium, the slow calcium signal was completely blocked (Fig. 5 *A*). Similar results were obtained using diltiazem and verapamil (data not shown). On the other hand, when myotubes were pretreated with the stimulatory dihydropyridine agonist (−)S-Bay K 8644, in the absence of extracellular calcium (Fig. 5 *A*), the slow calcium signal became faster than in the control condition ($t_{1/2}$ = 37.27 ± 2.56 and $t_{1/2}$ = 98.40 ± 7.92 s, respectively) together with a slight increase (20%) in the maximal fluorescence (Table 2). These results suggest that the active conformation of the DHPR is involved in the intracellular transduction to originate the slow calcium signal in response to high-frequency stimulation. To further verify the role of the DHPR as a voltage sensor, when a skeletal muscle cell line derived from dysgenic mice (GLT cell line) was subjected to the electrical protocol (Fig. 5 *B*), the lack of the $\alpha 1_S$ subunit of the DHPR was sufficient to abolish the slow calcium response. As a positive control, a cell line derived from wild-type mice (NLT cells) shows a slow calcium signal resembling that of primary myotubes. Furthermore, when a GLT clone stable-transfected with the DHPR-$\alpha 1_S$ subunit was exposed to the electrical stimulation the slow calcium signal was recovered, showing that the DHPR is essential to elicit the slow calcium signal.

TABLE 2 Slow calcium signal properties under different conditions

	Calcium	Calcium-free	TTX	Ryanodine*	Nifedipine*	Bay K*
$t_{1/2}$	54.34 ± 4.56 (12)	98.40 ± 7.92† (12)	NS (7)	66.61 ± 5.17‡ (10)	NS (13)	37.27 ± 2.56§ (16)
$(\Delta F/F_o)_{max}$	0.735 ± 0.079 (12)	0.733 ± 0.046 (12)	NS (7)	0.974 ± 0.073‡ (10)	NS (13)	0.880 ± 0.044‡ (16)

Values given represent mean ± SE (*n*); *NS*, no signal.
*Experiments performed in calcium-free media.
$^{\dagger}P < 0.01$ vs. calcium condition.
$^{\ddagger}P < 0.05$ vs. calcium-free condition.
$^{\S}P < 0.01$ vs. calcium-free condition.

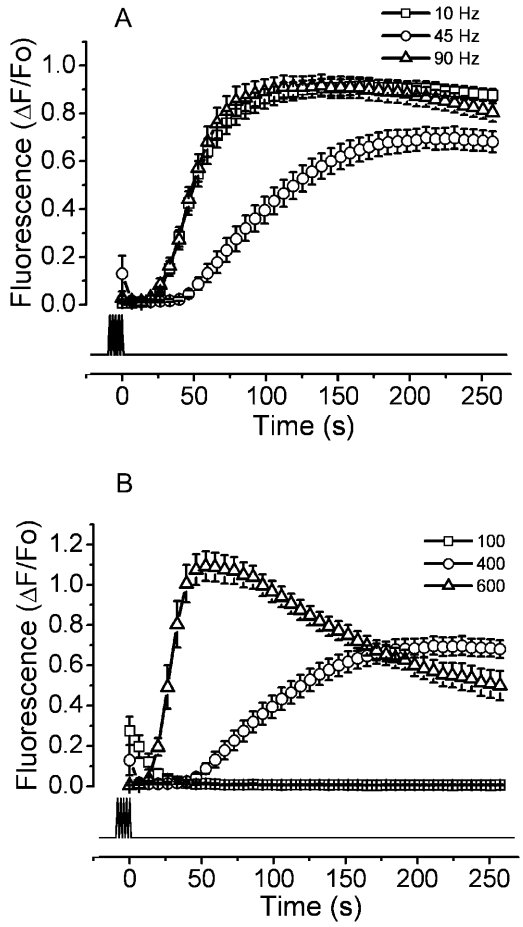

FIGURE 3 Variations in the frequency or number of pulses modify the shape of the slow calcium signal. The following protocols of electrical stimulation were used. (*A*) Different frequencies: the cells were exposed to 400 pulses of 1 ms at 10 Hz (*squares*), 45Hz (*circles*), or 90 Hz (*triangles*). (*B*) Different number of pulses: myotubes were exposed to 100 (*squares*), 400 (*circles*), or 600 (*triangles*) pulses of 1 ms at 45 Hz. All experiments were performed in the absence of extracellular calcium (0.5 mM EGTA added). The mean of at least 12 independent experiments ± SE is shown. The lower trace shows the duration of the stimulus protocol.

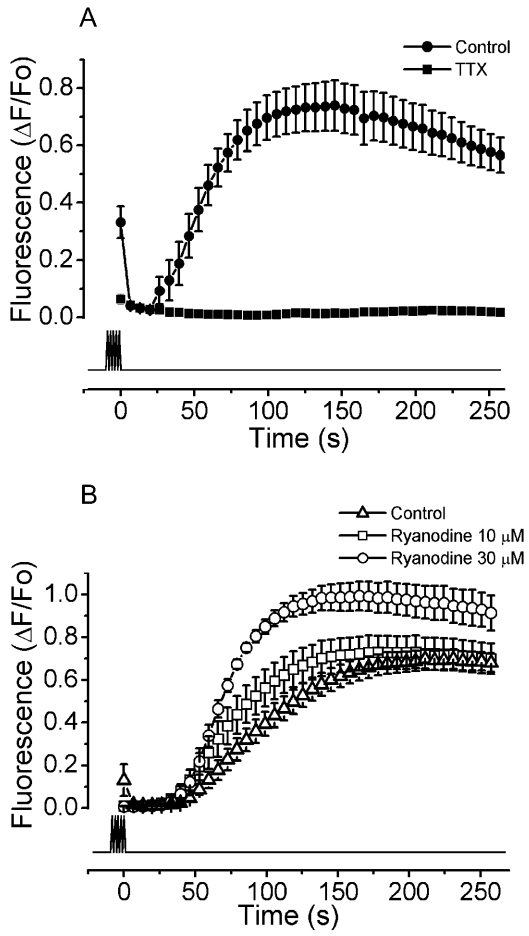

FIGURE 4 The slow calcium signal is blocked by TTX and is refractory to ryanodine. The myotubes were exposed to 400 pulses of 1 ms at 45 Hz. (*A*) The experiments were performed in normal saline with calcium (*solid circles*) and 10 μM TTX (*solid squares*). The mean of at least seven independent experiments ± SE is shown. (*B*) The fluorescence signals after the exposure to 10 μM (*open squares*) and 30 μM (*open circles*) of ryanodine, and the control condition without extracellular calcium (0.5 mM EGTA, *open triangles*), are shown. The mean of at least 10 independent experiments ± SE is shown. The lower trace shows the timing of the stimulation protocol.

Both PLC and IP_3 are involved in the slow calcium signal

A role of both PLC and IP_3 has previously been described for potassium depolarization-induced slow calcium signals (Jaimovich et al., 2000; Estrada et al., 2001). We measured the kinetics of IP_3 mass increase induced by electrical stimulation protocols. In Fig. 6 *A*, the comparative kinetics between IP_3 mass and calcium after electrical depolarization is shown. The mass of IP_3 shows a transient increase with a maximum 75 s after the end of stimulation, corresponding to a few seconds before the slow calcium signal peak was reached.

When the cells were exposed to 5 μM xestospongin C, a known blocker of IP_3R (Gafni et al., 1997), the maximum fluorescence of the slow calcium signal diminished from 0.733 ± 0.046 to 0.225 ± 0.045 $\Delta F/F_o$ (Fig. 6 *B*). This is 69.3% less than the control condition (Fig. 6 *B*).

To evaluate the role of PLC in the slow calcium signal, cultures were exposed to U73122, a PLC inhibitor, and then exposed to the electrical stimulation. This inhibitor diminished the maximal fluorescence from 0.980 ± 0.077 to 0.377 ± 0.049 $\Delta F/F_o$, which is a decrease of 61.5% from the control value (Fig. 6 *C*).

DISCUSSION

Our laboratory has previously shown that in myotubes, potassium depolarization elicits a fast, ryanodine-sensitive calcium transient related to EC coupling. This signal is followed by a second slow calcium transient, unrelated to

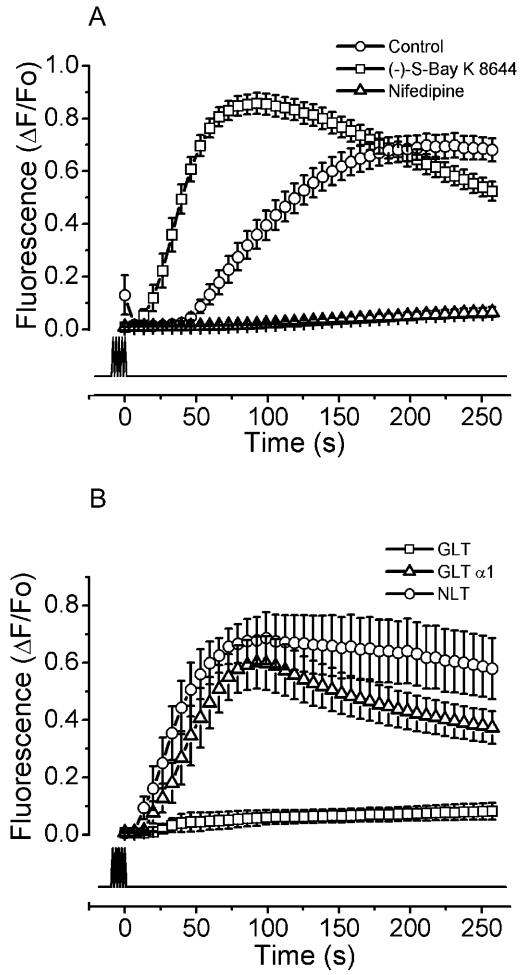

FIGURE 5 The DHPR is the membrane potential sensor for the slow calcium signal. Myotubes were stimulated with 400 pulses of 1 ms at 45 Hz. (*A*) The myotubes in nominally zero calcium (*open circles*) were exposed to 1 μM of (−)-S-Bay K 8644, a DHPR activator (*open squares*), and 1 μM nifedipine (*open triangles*). The mean for each condition of at least 13 independent experiments ± SE is shown. (*B*) Myotubes derived from the dysgenic skeletal muscle cell line (GLT, *open squares*), the wild-type mice derived cell line (NLT, *open circles*), and a GLT clone stable-transfected with the DHPR-$\alpha 1_S$ subunit (GLT-α1, *open triangles*) were exposed to the same stimulation protocol as described in *A*. The experiments were performed in the absence of extracellular calcium. The mean of at least six independent experiments ± SE for each condition is shown. The lower trace indicates the time of stimulation.

contraction, that depends on IP_3 receptors and can be related to regulation of gene expression (Jaimovich et al., 2000; Powell et al., 2001; Carrasco et al., 2003). Recently, a role for DHPRs as voltage sensors for the slow calcium signal induced by high potassium depolarization was proposed (Araya et al., 2003). In contrast to the electrical stimulation, the high potassium depolarization clamps the membrane voltage to a depolarized condition (Jaimovich and Rojas, 1994). When the voltage-gated channels are subjected to a prolonged period of depolarization, they will transit from closed to open and later to inactivated conformational states (Bezanilla, 2000) where, despite the positive membrane potentials, the channels will remain nonconductive until the resting potential is recovered. The model for the DHPR voltage sensing in skeletal muscle proposed by Rios and collaborators (Rios and Pizarro, 1991) gives a reference framework to follow the operational state of the channel. In it, the channel may be present in either active or inactive conformations. The closed-to-open transition in the active conformation gives rise to a Q1 type of charge movement and the closed-to-inactive conformation (nonconductive) gives rise to a Q2 type of charge movement. We do not know which conformational state or transition of the DHPR conveys the signaling for the slow calcium response, but the use of an external electrical field as stimulus to generate action potentials allows us to cycle the DHPR through its voltage-dependent kinetic states. Also, in contrast to the high potassium depolarization, it gives us the option of eliciting a controlled number of effective stimuli to the cell, which may mimic in part the motor unit activity.

To verify that the stimulation by itself was insufficient to elicit this type of response, we tested two different protocols, low-frequency and tetanic high-frequency stimulations. In both conditions the calcium transient induced during stimulation was completely blocked by TTX, showing that action potentials, and not the extracellular electrical field itself, trigger EC coupling. Moreover, the fast calcium transient was blocked by ryanodine as expected from the known physiological role of ryanodine receptors in EC coupling.

We have shown here that a tetanic stimulation generates an action potential-dependent slow calcium response. In our experimental conditions, we need >200 pulses (each pulse of 1 ms) with at least a 10-Hz repetition rate to obtain the characteristic slow response. The onset of this response occurs near 20–50 s after the end of the stimulation protocol and lasts for at least 5 min. Considering that the signal obtained by high potassium depolarization starts 3–4 s after the stimulus and lasts for 20–30 s (Jaimovich et al., 2000; Araya et al., 2003), it suggests that this delayed but enhanced slow calcium response originates from the activated rather than the inactivated state of the DHPR. In an effort to understand the relationship between stimulation frequency and slow calcium signals, we stimulated the myotubes with 400 pulses at 10, 45, and 90 Hz. Surprisingly, the onset kinetics for the slow signal at 10 and 90 Hz shows a very similar response, which is in both cases faster than the one present at 45 Hz. A plausible explanation for this result is that at 10 Hz the cell has enough time between pulses to repolarize completely, so that all the pulses elicit an action potential and the DHPR will be sensing each action potential and be reprimed afterwards. In contrast, at 45 Hz, even if the cell may generate all action potentials driven by the sodium channel, the DHPR, which has slower kinetics, may not fully recover from inactivation, becoming unable to sense every depolarization event, resulting in a delayed signal. On the

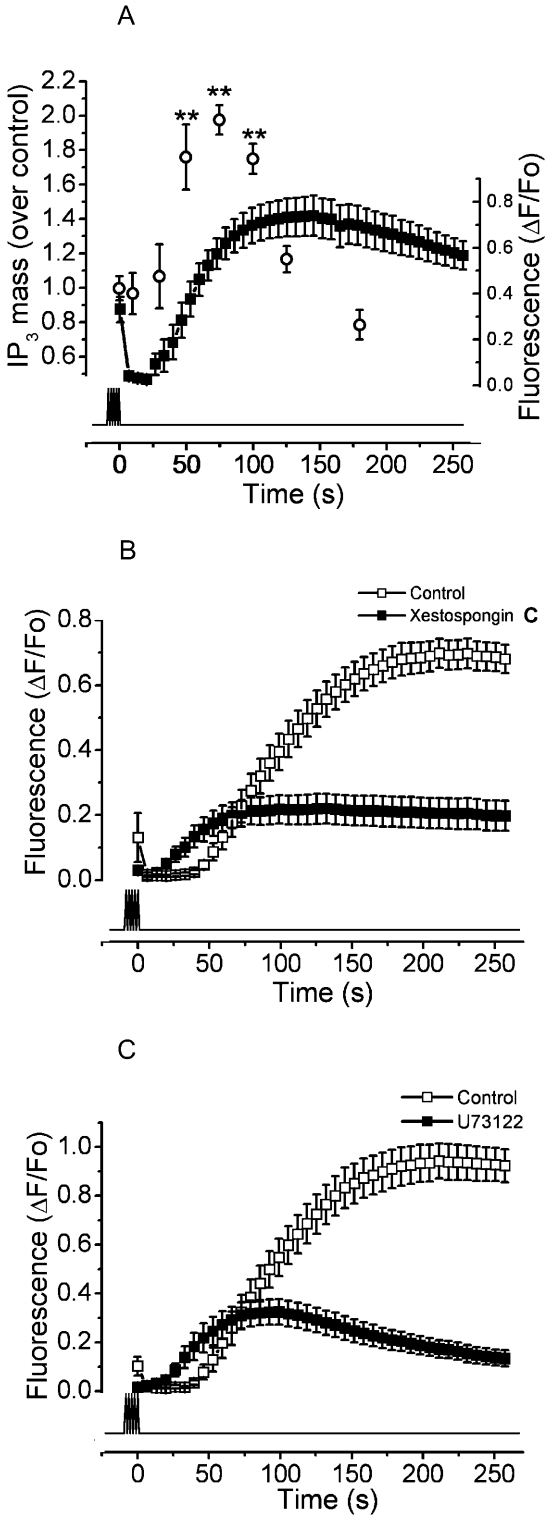

FIGURE 6 PLC and IP_3R are involved in the slow calcium signal. (*A*) The kinetics of IP_3 production induced by electrical stimulation is shown (*open circles*). Myotube cultures were exposed to 400 pulses of 1 ms at 45 Hz. Then IP_3 mass was measured as described in Materials and Methods. Each time point indicates the mean ± SE of three independent experiments. The difference in the response is statistically significant (**, $P < 0.01$) in comparison to the control condition. Superimposed is shown the slow calcium signal in the same temporal scale (*solid squares*) for the mean of 12 independent experiments ± SE for the same condition. (*B*) The slow calcium signal induced by electrical stimulation in the conditions described above was measured in the presence of the IP_3R blocker xestospongin C (*solid squares*); the control condition in the absence of extracellular calcium (0.5 mM EGTA) is shown (*open squares*). The mean of at least 12 independent experiments ± SE is shown. (*C*) Inhibition of the slow calcium signal in the presence of the PLC inhibitor U73122 (*solid squares*). The signal obtained for the control condition is also shown (*open squares*). In each case, the mean of at least 12 independent experiments ± SE is shown. The lower trace indicates the timing for the stimulation protocol.

other hand, at 90 Hz the cells may not generate all the action potentials (not enough time for sodium reactivation), which mimics a lower frequency stimulation.

The increase in the slow calcium response associated with the number of pulses at the same frequency of delivery indicates a temporal summation over the kinetics for the underlying process. This dose response-like phenomenon suggests that the effect on the voltage sensor can be additive at the cell level to allow modulation of the slow calcium response.

Interestingly, the nominal absence of extracellular calcium does not block the signal, implying that calcium comes from intracellular stores. The comparison of the calcium-free with the control condition shows that the absence of external calcium delays the signal without a change in the maximum fluorescence value. The kinetic differences between these two conditions may be explained by calcium influx during the beginning of the slow signal. Alternatively, the low calcium condition may shift the voltage activation curve of the DHPR (Brum et al., 1988), leaving fewer channels available for the active state. This will have a slow down propagation effect along the transductional pathway. One fact that supports the second explanation is that the maximum fluorescence in both conditions remains the same.

Under our experimental conditions, the slow calcium signal induced by electrical field stimulation is not blocked by ryanodine. This finding agrees well with the measured slow calcium responses in 1B5 cells (skeletal muscle cell line without RyR, data not shown), showing that as previously demonstrated for high potassium depolarization (Estrada et al., 2001), calcium released through IP_3Rs is responsible for the slow signal. The observed increase in $t_{1/2}$ and peak amplitude of the slow calcium signal at high ryanodine concentration may be related to the subconductance state at which the channel is left by the blocker that in turn could prime the overall calcium response.

To study in more detail the participation of the DHPR in the signal transduction path of the slow calcium signal, cells were exposed to an antagonist (nifedipine) and an agonist (−)S-Bay K dihydropyridine (Hockerman et al., 1997). In low calcium, nifedipine will have an additive effect of shifting the DHPR to the inactive state (Rios and Pizarro, 1991; Squecco et al., 2004), also seen as a decrease in force generation (Dulhunty and Gage, 1988). Our results show that nifedipine completely blocks the slow calcium signal,

supporting the notion that this molecule's voltage sensor is the structural feature that interfaces the membrane depolarization and the release of calcium through the IP_3R to generate the slow calcium signal. Interestingly, Bay K strongly accelerates the slow calcium signal $t_{1/2}$ with an increase of the maximum fluorescence (Table 2), which correlates well with its known action of increase in open channel probability (Hess et al., 1984). This agent also shows a voltage-dependent antagonistic action, shifting and lowering the crisscrossing point to the left of the voltage axis (Artigas et al., 2003). In our experimental conditions, the fraction of the sensors bound to the drug in an inactivated conformation will reduce the availability of the Q1 receptors, but the remaining activated channels (charge 1) will have a favored kinetics toward the open state, enhancing the transductional effect on the slow calcium signal onset.

Another fact that supports the DHPR role in the slow calcium signal is the complete absence of response in electrically stimulated myotubes derived from the dysgenic cell line (GLT). In contrast, myotubes derived from both the normal cell line (NLT) and the cells stable-transfected with the $\alpha 1_S$ subunit to the GLT cell line (GLT-α1) present the slow calcium response. All together, this data strongly suggests that the active conformation of the DHPR induced by membrane depolarization activates in turn the IP_3 signal transduction mechanism for the development of the slow calcium signal.

Previous reports from our laboratory have shown that the potassium depolarization induces the IP_3 increase by PLC activation that in turn activates the IP_3R involved in the slow calcium release (Jaimovich et al., 2000; Estrada et al., 2001). Also we have reported that IP_3Rs are present in the skeletal myotubes; interestingly enough, they are placed in the perinuclear region and the sarcoplasmic reticulum (Jaimovich et al., 2000; Powell et al., 2001). This placement may explain the cytosolic and nuclear components of the slow calcium signal induced by electrical stimulation. To verify the role of the PLC in the slow calcium signal induced by electrical stimulation, we measured the kinetics of IP_3 mass production. The IP_3 curve shows a twofold increase in mass with respect to the control condition, which correlates very well with the calcium signal kinetics described in this work (Fig. 6 *A*). This result gives additional support to the notion that IP_3 may be the second messenger involved in development of slow calcium signals. The comparison of the kinetics of IP_3 mass previously described for potassium depolarization with those described here presents some differences that may reflect the procedural origin of those kinetics. The potassium-induced change has two peaks, one at 2–3 s and another at 15 s after the onset of depolarization. Then, the IP_3 amount returns to the basal levels between 50 and 60 s in the high-potassium condition (Jaimovich et al., 2000). Meanwhile, the electrically stimulated cells present a single component that starts after 30 s and finishes 100–125 s after the stimulus ends. These kinetic differences do explain the different shapes of slow calcium signals for both conditions.

To further evaluate the role of IP_3 as the agonist in the generation of the slow calcium signal, myotubes were exposed to xestospongin C, an IP_3R blocker; this agent strongly inhibited the maximum fluorescence (69.3% with respect to the control condition, Fig. 6 *B*). In addition, treatment of myotubes with U73122, an inhibitor of PLC, also strongly inhibited the signal. These results support the idea of PLC activation after electrical stimulation. The inhibitory effect found with these agents points toward the participation of both PLC and IP_3 as the main mechanism for calcium release during the slow calcium signal induced by electrical stimulation, corroborating what was previously described for potassium depolarization (Estrada et al., 2001).

Kinetically, in the presence of inhibitors there appears to be a shorter delay for the onset of the slow calcium rise compared with control conditions. This observation suggests, on one hand, that an IP_3-insensitive component may be present and, on the other, that the IP_3 system is also necessary to explain the delay observed in these signals.

Recently we have described (Araya et al., 2003) how the high potassium-induced slow calcium signal is pertussis toxin-sensitive, indicating the possible participation of the trimeric Gi protein as a molecular transducer between DHPR and PLC. The PLC family includes 11 isoenzymes that have been divided into four groups: four PLC-β, two PLC-γ, four PLC-δ, and the recently identified PLC-ε. Each PLC group has different modules that give a singular activation mechanism (Rebecchi and Pentyala, 2000; Rhee, 2001). In particular, all PLC-β isoforms can be activated by both Gαq or G$\beta\gamma$ released from the Gi trimer. One speculative mechanism of depolarization-induced PLC activation would involve the participation of G$\beta\gamma$ and PLCβ, but further studies must be performed to elucidate this process.

In summary, this work clearly shows that the slow calcium signal is an event driven by DHPR in response to repetitive activation of its intrinsic voltage-sensing structure. This slow signal does not contribute to the cell contraction; indeed, the maximal fluorescence obtained for the slow signal is less than one-half that obtained during the fast calcium transient in the same experiment (data not shown). Thus, the cytosolic calcium concentration reached during the RyR-dependent signal is much larger than the concentration reached during the IP_3R-dependent signal. Nevertheless, the extended time course of the slow calcium signal, in particular at the nucleus, may modulate the calcium-dependent signal pathways involved in cellular homeostasis and adaptation to environmental changes relayed by the degree of electrical activity at the sarcolemma.

The authors thank Monica Silva for cell culture preparation and Susana Vargas and Roni Silvestre for preliminary data.

Financial support from a Comisión Nacional de Investigación Científica y Tecnológica predoctoral fellowship to J.M.E. and a Fondo Nacional de Investigación en Áreas Prioritarias project grant (15010006) is also acknowledged.

REFERENCES

Araya, R., J. L. Liberona, J. C. Cardenas, N. Riveros, M. Estrada, J. A. Powell, A. Carrasco, and E. Jaimovich. 2003. Dihydropyridine receptors as voltage sensors for a depolarization-evoked, IP_3R-mediated, slow calcium signal in skeletal muscle cells. *J. Gen. Physiol.* 121:3–16.

Artigas, P., G. Ferreira, N. Reyes, G. Brum, and G. Pizarro. 2003. Effects of the enantiomers of BayK 8644 on the charge movement of L-type Ca channels in guinea-pig ventricular myocytes. *J. Membr. Biol.* 193:215–227.

Bezanilla, F. 2000. The voltage sensor in voltage-dependent ion channels. *Physiol. Rev.* 80:555–592.

Brum, G., R. Fitts, G. Pizarro, and E. Rios. 1988. Voltage sensors of the frog skeletal muscle membrane require calcium to function in excitation-contraction coupling. *J. Physiol.* 398:475–505.

Carrasco, M. A., N. Riveros, J. Rios, M. Muller, F. Torres, J. Pineda, S. Lantadilla, and E. Jaimovich. 2003. Depolarization-induced slow calcium transients activate early genes in skeletal muscle cells. *Am. J. Physiol. Cell Physiol.* 284:C1438–C1447.

Catterall, W. A. 2000. Structure and regulation of voltage-gated Ca^{2+} channels. *Annu. Rev. Cell Dev. Biol.* 16:521–555.

Curtis, B. M., and W. A. Catterall. 1984. Purification of the calcium antagonist receptor of the voltage-sensitive calcium channel from skeletal muscle transverse tubules. *Biochemistry.* 23:2113–2118.

Dulhunty, A. F., and P. W. Gage. 1988. Effects of extracellular calcium concentration and dihydropyridines on contraction in mammalian skeletal muscle. *J. Physiol.* 399:63–80.

Ertel, E. A., K. P. Campbell, M. M. Harpold, F. Hofmann, Y. Mori, E. Perez-Reyes, A. Schwartz, T. P. Snutch, T. Tanabe, L. Birnbaumer, R. W. Tsien, and W. A. Catterall. 2000. Nomenclature of voltage-gated calcium channels. *Neuron.* 25:533–535.

Estrada, M., C. Cárdenas, J. L. Liberona, M. A. Carrasco, G. A. Mignery, P. D. Allen, and E. Jaimovich. 2001. Calcium transients in 1B5 myotubes lacking ryanodine receptors are related to inositol trisphosphate receptors. *J. Biol. Chem.* 276:22868–22874.

Gafni, J., J. A. Munsch, T. H. Lam, M. C. Catlin, L. G. Costa, T. F. Molinski, and I. N. Pessah. 1997. Xestospongins: potent membrane permeable blockers of the inositol 1,4,5-trisphosphate receptor. *Neuron.* 19:723–733.

Grabner, M., R. T. Dirksen, N. Suda, and K. G. Beam. 1999. The II–III loop of the skeletal muscle dihydropyridine receptor is responsible for the bi-directional coupling with the ryanodine receptor. *J. Biol. Chem.* 274:21913–21919.

Hartree, E. F. 1972. Determination of protein: a modification of the Lowry method that gives a linear photometric response. *Anal. Biochem.* 48:422–427.

Hess, P., J. B. Lansman, and R. W. Tsien. 1984. Different modes of Ca channel gating behaviour favoured by dihydropyridine Ca agonists and antagonists. *Nature.* 311:538–544.

Hockerman, G. H., B. Z. Peterson, B. D. Johnson, and W. A. Catterall. 1997. Molecular determinants of drug binding and action on L-type calcium channels. *Annu. Rev. Pharmacol. Toxicol.* 37:361–396.

Jaimovich, E., R. Reyes, J. L. Liberona, and J. A. Powell. 2000. IP_3 receptors, IP_3 transients, and nucleus-associated Ca^{2+} signals in cultured skeletal muscle. *Am. J. Physiol. Cell Physiol.* 278:C998–C1010.

Jaimovich, E., and E. Rojas. 1994. Intracellular Ca^{2+} transients induced by high external K^+ and tetracaine in cultured rat myotubes. *Cell Calcium.* 15:356–368.

Kasielke, N., G. J. Obermair, G. Kugler, M. Grabner, and B. E. Flucher. 2003. Cardiac-type EC-coupling in dysgenic myotubes restored with Ca^{2+} channel subunit isoforms α_{1C} and α_{1D} does not correlate with current density. *Biophys. J.* 84:3816–3828.

Kubis, H. P., N. Hanke, R. J. Scheibe, J. D. Meissner, and G. Gros. 2003. Ca^{2+} transients activate calcineurin/NFATc1 and initiate fast-to-slow transformation in a primary skeletal muscle culture. *Am. J. Physiol. Cell Physiol.* 285:C56–C63.

Liberona, J. L., J. A. Powell, S. Shenoi, L. Petherbridge, R. Caviedes, and E. Jaimovich. 1998. Differences in both inositol 1,4,5-trisphosphate mass and inositol 1,4,5-trisphosphate receptors between normal and dystrophic skeletal muscle cell lines. *Muscle Nerve.* 21:902–909.

Powell, J. A., M. A. Carrasco, D. S. Adams, B. Drouet, J. Rios, M. Muller, M. Estrada, and E. Jaimovich. 2001. IP_3 receptor function and localization in myotubes: an unexplored Ca^{+2} signaling pathway in skeletal muscle. *J. Cell Sci.* 114:3673–3683.

Powell, J. A., L. Petherbridge, and B. E. Flucher. 1996. Formation of triads without the dihydropyridine receptor α-subunits in cell lines from dysgenic skeletal muscle. *J. Cell Biol.* 134:375–387.

Proenza, C., J. O'Brien, J. Nakai, S. Mukherjee, P. D. Allen, and K. G. Beam. 2002. Identification of a region of RyR1 that participates in allosteric coupling with the α_{1S} ($Ca_V1.1$) II–III loop. *J. Biol. Chem.* 277:6530–6535.

Rasband, W. S. 1997. ImageJ, National Institutes of Health, Bethesda, Maryland. http://rsb.info.nih.gov/ij.

Rebecchi, M. J., and S. N. Pentyala. 2000. Structure, function, and control of phosphoinositide-specific phospholipase C. *Physiol. Rev.* 80:1291–1335.

Rhee, S. G. 2001. Regulation of phosphoinositide-specific phospholipase C. *Annu. Rev. Biochem.* 70:281–312.

Rios, E., and G. Pizarro. 1991. Voltage sensor of excitation-contraction coupling in skeletal muscle. *Physiol. Rev.* 71:849–908.

Squecco R., C. Bencini, C. Piperio, and F. Francini. 2004. L-Type Ca^{2+} channel and ryanodine receptor cross-talk in frog skeletal muscle. *J. Physiol.* 555:137–157.

Tanabe, T., K. G. Beam, B. A. Adams, T. Niidome, and S. Numa. 1990. Regions of the skeletal muscle dihydropyridine receptor critical for excitation-contraction coupling. *Nature.* 346:567–569.

Wolf, M., A. Eberhart, H. Glossmann, J. Striessnig, and N. Grigorieff. 2003. Visualization of the domain structure of an L-type Ca^{2+} channel using electron cryo-microscopy. *J. Mol. Biol.* 332:171–182.